Hsa-circRNA-G004213 promotes cisplatin sensitivity by regulating miR-513b-5p/PRPF39 in liver cancer

LING QIN, ZIBO ZHAN, CHUNXUE WEI, XUEMEI LI, TONGQIN ZHANG and JUN LI

Department of Gastroenterology, Clinical Medical College and The First Affiliated Hospital of Chengdu Medical College, Chengdu, Sichuan 610000, P.R. China

Received September 15, 2020; Accepted March 1, 2021

DOI: 10.3892/mmr.2021.12060

Abstract. In recent years, increasing evidence has confirmed that exosomal circular RNAs (circRNAs) serve a crucial role in the prognostic prediction and diagnosis of liver cancer (LC). The present study compared the expression patterns of exosomal circRNAs during transarterial chemoembolization (TACE). CircRNA sequencing analysis identified 390 differentially expressed circRNAs between the prior TACE and following the first TACE operation groups and 489 differentially expressed circRNAs between the prior to TACE and following the second TACE operation groups. Gene Ontology analysis of the differentially expressed circRNAs demonstrated that they were associated with fatty acid metabolism, receptor binding and membrane protein complexes. Kyoto Encyclopedia of Genes and Genomes pathway analysis predicted that protein digestion and absorption pathways were activated following TACE. A novel gene was screened out; hsa-circRNA-G004213 (circ-G004213) was significantly upregulated following TACE (fold change >10, P<0.01). Further analysis found circ-G004213 significantly increased the cisplatin sensitivity of HepG2 cells and positively associated with the prognosis of tumor-bearing mice. Based on the potential downstream miRNAs and mRNAs, the circRNA-miRNA-mRNA network was constructed. It was demonstrated that circ-G004213 regulated cisplatin resistance via the miR-513b-5p/PRPF39 axis. Finally, the present study confirmed that circ-G004213 was positively associated with the prognosis of patients with LC following TACE. Therefore, circ-G004213 may be used as an indicator for predicting the efficacy of TACE.

Correspondence to: Dr Jun Li, Department of Gastroenterology, Clinical Medical College and The First Affiliated Hospital of Chengdu Medical College, 278 Bao Guang Road, Xindu, Chengdu, Sichuan 610000, P.R. China
E-mail: 84183967@qq.com

Abbreviations: LC, liver cancer; TACE, transarterial chemoembolization; circ-G004213, hsa-circRNA-G004213; mRNA, messenger RNA; miRNA, microRNA; lncRNA, long noncoding RNA; circRNA, circular RNA; prior TACE, prior to TACE treatment; TACE1, after the first TACE operation; TACE2, after the second TACE operation; TEM, transmission electron microscope; MNNA, Malvern Nano-Nano Analyzer; CIS, cisplatin; RT-qPCR, reverse transcription-quantitative PCR; HBV, hepatitis virus B; AFP, alpha-fetoprotein; GO, Gene Ontology; BP, biological process; CC, cell component; MF, molecular function; KEGG, Kyoto Encyclopedia of Genes and Genomes; NC, negative control; OE, overexpression

Key words: exosomes, circular RNAs, cisplatin, liver cancer, transarterial chemoembolization

Introduction

Globally, liver cancer (LC) is the commonest type of hepatic malignancy and the third leading cause of cancer-related death (1). Transarterial chemoembolization (TACE) is mainly used to treat unresectable advanced LC and can also be used for complementary treatment without radical resection. As most patients with LC are diagnosed at advanced stages, which causes them to miss the best opportunity for curative therapy via resection, transplantation or ablation, TACE serves an important role in the treatment of LC. The main mechanism of the treatment of LC relies on the difference in the blood supply between LC and normal liver tissue. A total of 95-99% of the LC blood supply is derived from the hepatic artery and 70-75% of the liver tissue blood supply is derived from the portal vein (2). TACE can effectively block the blood supply from the hepatic artery while continuously releasing high-concentration chemotherapy drugs (cisplatin and fluorouracil) to directly kill tumor cells and has little effect on normal liver tissue (3). Tumor stage, portal hypertension and preoperative levels of α fetoprotein, alkaline phosphatase, γ glutamyl transpeptidase and monocytes are important clinical indicators to predict the efficacy of TACE (4). Serum IL-6 and IL-8 levels may help to identify patients who benefit from TACE in terms of objective response to treatment and overall survival before intervention (5). Circulating MMP-2 is also associated with the prognosis of LC following TACE (6). However, molecular markers of TACE-related prognostic indicators are lacking.

Exosomes are microcapsule structures with a lipid bilayer having a diameter of 30-150 nm that are secreted by various normal cells and tumor cells and are naturally present in various body fluids (7). They contain proteins, lipids, messenger RNA (mRNA), microRNA (miRNA), long noncoding RNA (lncRNA), circular RNA (circRNA) and

transcription factors (8,9). Exosomes serve a crucial role in the carcinogenesis of LC (10,11).

In the process of carcinogenesis, exosomes are associated with viral spread and affect host immunity, which causes DNA damage and LC. For example, exosomal miR-122 promotes viral RNA replication and transmission between hepatitis virus C-infected hepatocytes and normal hepatocytes via the AGO2-miR-122-HSP90 complex (12). lncRNA FAL1/miR-1236 can promote tumor metastasis (13). Noncoding (nc)RNAs can be transferred to immune cells through exosomes to induce the expansion or differentiation of immunosuppressive cells in LC. For example, exosomal miR-23a-3p can upregulate the expression of programmed death-ligand 1 through the PTEN-PI3K/AKT pathway (14).

An increasing number of studies have demonstrated that exosomal circRNAs serve a key role in the prediction and diagnosis of LC. For example, exosomal circRNA-100338 can promote LC metastasis (15). The circRNA Cdr1, as a competitive endogenous RNA, is associated with the progression of LC (16). Exosomal circPTGR1 promotes LC metastasis via the miR449a-hepatocyte growth factor receptor (MET) pathway (17). In addition, exosomal circRNAs secreted from adipocytes can promote the growth of LC by targeting the deubiquitination-related protein USP7 (18).

The present study first compared the expression patterns of exosomal circRNAs during TACE. Hepatic artery blood was collected from 5 patients with LC at three time points: Prior to TACE treatment (prior TACE), following the first TACE operation (TACE1) and following the second TACE operation (TACE2). Then, the exosomes were extracted from the blood and the alterations of the circRNAs in exosomes were further analyzed. A novel circRNA was screened (circ-G004213). The present study demonstrated that circ-G004213 was associated with the prognosis of patients with LC. By constructing circRNA-miRNA-mRNA interaction, it was found that circ-G004213 interacted with miR-513b-5p and downstream target gene PRPF39. Previous studies found that miR-513b-5p can suppress cell promotion in experimental electromagnetic cancer cells and suppress cell promotion and migration in ovarian cancer (19,20). In addition, PRPF39 was associated with cisplatin sensitivity (21). The present study was performed in order to further confirm the role and mechanism of circ-G004213/miR-513b-5p/PRPF39 in the cisplatin sensitivity of LC.

Materials and methods

Human specimens. Hepatic artery blood was collected from five male patients between May 2017 and May 2019 with LC (age range between 26 and 66 years old) at three time points: Prior TACE, TACE1 and TACE2. A total of 10 ml of hepatic artery blood was drawn from each patient at each time point, EDTAK2 was used to anticoagulant and the plasma was separated (2,000 x g, 10 min at 4˚C) and immediately frozen at -80˚C prior to the extraction of exosomes. All five patients were enrolled from the Department of Gastroenterology at the First Affiliated Hospital of Chengdu Medical College (Chengdu, China) from 2018-2019. The other 50 patients with LC' blood samples were obtained from the tissue specimen bank of the First Affiliated Hospital of Chengdu Medical College (2017-2020; Table I). LC was diagnosed according to the 2017 specifications for the diagnosis and treatment of primary liver cancer using TNM and Barcelona Clinic Liver Cancer staging (BCLC) tumor staging assessment (22). Child-Pugh score was used to evaluate the changes in liver function of the patients following TACE treatment (23). None of the patients with LC received chemotherapy or radiotherapy before TACE. The clinical, imaging and pathologic records of the patients were reviewed retrospectively. Informed consent was signed in writing by all patients and the study protocol was approved by the ethics committee of the First Affiliated Hospital of Chengdu Medical College (approval no. 2017009).

Isolation of exosomes. Exosomes in plasma were separated by an exoEasy Maxi kit (Qiagen China Co., Ltd.). XBP buffer (3 ml) was added to 3 ml of plasma. The centrifuge tube was immediately inverted gently to mix the solution and kept at room temperature. The plasma/XBP buffer mixture was then added to the exoEasy rotary column and centrifuged at 500 x g for 1 min at 4˚C. The flow through was discarded and the rotating column was placed in the same collecting tube. XWP buffer (10 ml) was added and centrifuged at 5,000 x g for 5 min at 4˚C to remove the residual volume from the rotating column. All the flow through in the collection tube was discarded. The rotating column was moved into a new collecting tube. Next, 400 μl-1 ml of Xe buffer was added to the membrane and incubated for 1 min at 4˚C. The test tube was centrifuged at 500 x g for 5 min at 4˚C and the eluate was collected. Finally, the eluate was added to the exoEasy rotary column and incubated for 1 min and the tube was centrifuged at 5,000 x g for 5 min at 4˚C; then, the eluate was collected and transferred to a new collection tube. Finally, the exons were resuspended in PBS and stored at -80˚C.

Detection of exosomes. Exosomes were detected by three methods. First, exosomes were observed under a transmission electron microscope (TEM; HT7700; Hitachi, Ltd.). For an enhanced view of the plasma membrane, the exosomes were embedded in polymer at 65˚C for 48 h. Then, they were stained with uranium acetate for 10 min and lead acetate for 10 min (room temperature).

Western blotting was used to detect the typical exosomal markers, as below. Equal amounts of protein were subjected to SDS-PAGE. The protein extracted from blood was used as the control. The sources and dilutions of the antibodies that were used were as follows: Mouse anti-CD9 (Abcam; 1:400), mouse anti-CD63 (Abcam; 1:400), rabbit anti-tumor susceptibility gene (TSG)101 (Abcam; 1:1,000) and mouse anti-β-actin (Abcam; 1:1,000), which was used as an internal control. Finally, the exosomes were tested with a Malvern Nano-Nano Analyzer (MNNA; Nanosight NS300; Malvern Instruments, Ltd.) to measure their size.

CircRNA sequencing analysis. High-throughput full transcriptome sequencing and subsequent bioinformatics analysis were performed. According to the manufacturer's instructions, the RNA library was constructed with rRNA-depleted RNA using the TruSeq Stranded Total RNA library preparation tool (Illumina, Inc.). The Bioanalyzer 2100 system (Agilent Technologies, Inc.) was used to test and quantify the quality

Table I. Association between clinicopathological variables and circ-G004213 expression in patients with LC following TACE.

		circ-G004213		
Characteristics	Number	High	Low	P-value
Sex				0.496
Male	39	18	21	
Female	11	7	4	
Age (years)				0.999
≤50	8	3	5	
>50	42	19	23	
HBV				0.716
Positive	41	23	18	
Negative	9	6	3	
AFP (ng/ml)				0.033[a]
≤200	7	6	1	
>200	43	15	28	
TNM stage				0.009[a]
I and II	21	15	6	
III and IV	29	9	20	
BCLC stage				0.022[a]
A and B	23	16	7	
C and D	27	9	18	
Child-Pugh score				0.484
5-6	29	16	13	
7-9	18	7	11	
≥10	3	1	2	

HBV, hepatitis virus B; AFP, alpha-fetoprotein; BCLC, Barcelona Clinic Liver Cancer staging. [a]Significant difference.

of the library. A total of 10 picomolar libraries were denatured to generate single-stranded DNA molecules. These molecules were captured on Illumina flow cells and amplified *in situ* in clusters. Finally, 150 cycles of sequencing were performed on an Illumina HiSeq 4000 sequencer (Illumina, Inc.) according to the manufacturer's instructions. Paired end readings were taken from the Illumina HiSeq 4000 sequencer (Illumina, Inc.). After trimming of the 3' adapter, low-quality readings were removed by Cutadapt software (v1.9.3; https://pypi.python.org/pypi/cutadapt#downloads). High quality trim reading analysis was then performed. Star software (http://www.star-softwarein.com/) was used to compare high-quality reading data with the reference genome/transcriptome, DCC software (https://www.hpc.dtu.dk/? page_id=3270) was used to detect and identify circRNAs and the circRNA database (v0.1; http://www.circbase.org/.) was used for annotation. The data were normalized by edgeR software (v3.12; http://bioconductor.org/biocLiteR) and differential expression was analyzed. The relevant data of the present study have been uploaded to GEO depository with the number GSE 165183. Gene Ontology (GO) was used to study the differentially expressed molecules (http://www. http://geneontology.org). The Kyoto Encyclopedia of Genes and Genomes (KEGG; http://www.genome.jp/kegg) database was also used. Based on the GO and KEGG pathway analyses, the differentially expressed circRNAs were annotated and their functions determined.

Cell culture. The human 293T cells and LC cell lines HepG2 were derived from Wuhan tumor cell lines in China (Procell Life Science & Technology Co., Ltd.). HepG2 and 293T cells were identified by STR analysis. Mycoplasma conjugation test was performed in all cells and these cells have been used in our previous study (24). The acisplatin-resistant subline (HepG2/CIS) of HepG2 cells was established by repeated subculture in cisplatin (25). Cisplatin was purchased from Sigma-Aldrich (Merck KGaA) and dissolved in dimethyl sulfoxide to obtain a 10 mM stock solution. All cells were cultured in DMEM (HyClone; Cytiva) containing 10% fetal bovine serum (FBS, HyClone; Cytiva) and preserved at 37˚C and 5% CO_2. For comparison of the IC_{50} values of CIS among the groups of HepG2 cells, cell viability was evaluated through MTT assays as described previously (24). HepG2 cells ($1x10^4$) were plated in 96-well plates. Once the cells reached 70% confluence, CIS (0, 5, 10, 20, 40, 100 and 200 μM) was added. After the cells were incubated for an additional 72 h, the MTT reagent was added and allowed to incorporate for 4 h. The optical density at 570 nm was determined using an ELISA plate reader (Model 550; Bio-Rad Laboratories, Inc.).

Plasmid construction and transfection. For overexpression of circ-G004213, the full-length 339 bp cDNA of circ-G004213 was cloned into the vector pLCDH. The circ-G004213 and 2581-bp to 2600-bp fragments of PRPF39 were amplified from the cDNA of HepG2 cells and cloned into pmiRGLO (Promega Corporation) for luciferase analysis. All constructed plasmids were confirmed by sequencing. In addition, HepG2 cell lines with stable overexpression or knockout of PRPF39 were constructed with lentiviral vectors (24,25). Short interfering (si)RNA, miRNA mimics or inhibitors were synthesized by Guangzhou RiboBio Co., Ltd. siRNA-circ-G004213, 5'-AGA UUCUUAGACUCCAGAU-3'; siRNA-NC (negative control), 5'-UUCUCCGAACGUGUCACGU-3'. HepG2 cells were seeded in a six-well plate, and 100 pM of siRNA-circ-G004213 was transfected into HepG2 cells using TurboFect transfection reagent (Thermo Fisher Scientific, Inc.). miRNA mimics or inhibitors (Beckman Coulter, Inc.) were diluted to a final concentration of 20 nM in serum-free DMEM (HyClone; Cytiva). For transient transfection, HepG2 and 293T cells were transfected with Lipofectamine® 2000 (Invitrogen; Thermo Fisher Scientific, Inc.) according to the manufacturer's instructions. There was an interval of 24 h between transfection and subsequent experiments.

Luciferase reporter assay. Double fluorescein reporter gene detection was carried out according to the manufacturer's instructions (24,25). The Wild-type (WT) and mutant (MUT) circ-G004213 UTRs and PRPF39 UTRs were amplified and cloned into pmirGLO (Promega Corporation). For dual luciferase assays, 293T cells were cotransfected with the pmirGLO plasmid and miR-523b-5p mimic and pRLTK reporter gene carrier, respectively, with assistance of Lipofectamine® 2000 (Invitrogen; Thermo Fisher Scientific, Inc.). The firefly and *Renilla* luciferase activities were measured by applying dual

luciferase reporter assay system (Promega Corporation) 48 h following transfection according to the manufacturer's instructions. The luciferase activity was measured by a Multi-Mode Microplate Reader (Synergy 2; BioTek Instruments, Inc.). All the assays were repeated at least 3 times.

In vivo experiments. A total of 120 6-week-old BALB/c nude mice from Chengdu Dossy. Experimental Animal Co., Ltd. were subcutaneously inoculated in the flank region with HepG2 cells ($5x10^6$; circ-G004213-OE, vector-NC, si-circ-G004213 or si-NC). Then 10 mice in each group were subcutaneously injected with the cell mixture. The mice were fed in SPF animal center of Chengdu Medical College with the humidity at 50%, the temperature at 25˚C and 14-h light/10-h dark cycle. The tumor volume was calculated using the following formula: Tumor volume (mm^3)=π/6 x length x $width^2$. When the tumor volume reached 100 mm^3, CIS (10 μM) was intraperitoneally injected (25). The endpoint was tumors up to 1,000 mm^3. When they reached the endpoint, the mice were euthanized with 100% CO_2 with a flow rate of 40% and the endpoint was recorded. The animal experiments were approved by the research ethics committee of Chengdu Medical College (approval no. 2017CYA-021).

CircRNA-miRNA-mRNA interactions. To further study the relationship between circRNAs and miRNAs, the miRanda and TargetScan databases (http://www. microrna. org/microrna/home.do) were used to identify targeted miRNAs. From these predictions it was hypothesized that the circRNAs might act as miRNA sponges. Based on the binding sites of differentially expressed circRNAs and miRNAs, a network between circRNAs and miRNAs was constructed. According to the reverse splicing site coordinates of circRNAs, the coordinates of mRNAs (defined as circRNA-related genes) were found through the RefSeq database (v34; https://www. ncbi.nlm.nih.gov/refseq/).

Reverse transcription-quantitative (RT-q) PCR. To detect the expression of circRNAs and mRNA, RT-qPCR was performed according to the manufacturer's protocols. Total RNA from blood samples lysates was isolated using TRIzol® reagent (Thermo Fisher Scientific, Inc.). cDNA was synthesized with the PrimeScript RT Master Mix (Takara Biotechnology Co., Ltd.) from 500 ng RNA. The PCR analyses were performed with SYBR Premix Ex TaqII (Takara Biotechnology Co., Ltd.) with Light Cycler 480 II Real-Time PCR System (Roche Diagnostics). PCR protocol consisted of one cycle at 95˚C for 10 sec followed by 40 cycles at 95˚C for 5 sec and at 60˚C for 45 sec. The relative gene expression data was analyzed by the $2^{-\Delta\Delta Cq}$ method (26). GAPDH was used as an endogenous control gene for circRNAs and mRNA. To determine the abundance of circRNA, the divergent primers were designed for the circular transcripts. Primers for circRNAs and related mRNAs are shown in Table SI.

miR-4677-3p (Assay ID ap04309), miR-513b-5p (Assay ID ap002658), miR-580-3p (Assay ID ap01950), miR-219a-1-3p (Assay ID ap01258) and miR-6888-3p (Assay ID ap08601) were detected according to the RT-qPCR. Mir-X miRNA First-Strand Synthesis Kit (Takara Biotechnology Co., Ltd.) was used to reverse transcribe total RNA into mature miRNA. U6 was used as an endogenous control for miRNA expression analysis. Magnetic Resonance Elastography (MRE) was used for analysis. The threshold cycle (Cq) was defined as the fractional cycle number at which the fluorescence passed the fixed threshold. All assays were performed in triplicates.

Western blot analysis. Proteins from HepG2 transplanted tumor were extracted with common protein extraction reagent (Beyotime Institute of Biotechnology) and 1% phenylmethylsulfonyl fluoride. Protein concentrations were determined by BCA using an assay kit (Bio-Rad Laboratories, Inc.). Protein lysates (50 μg) were loaded by 4% sodium dodecyl sulfate-polyacrylamide gel and separated by 10% gel electrophoresis and transferred onto a polyvinylidene difluoride membrane (EMD Millipore). Membranes were incubated in blocking buffer (Tris-buffered saline containing 5% skimmed milk) for 1 h at 37˚C. The antibodies used were as follows: β-actin (cat. no. 8H10D10; Cell Signaling Technology, Inc.) PRPF39 (cat. no. PA5-21627; Invitrogen; Thermo Fisher Scientific, Inc.). The dilution factor of all antibodies was 1:1,000. The first antibody were incubation at 4˚C overnight. After washing, the membranes underwent hybridization with horseradish peroxidase-conjugated secondary antibody horseradish peroxidase conjugated anti-rabbit IgG (1:3,000; cat. no. 14708; Cell Signaling Technology, Inc.) and anti-mouse IgG (1:3,000; cat. no. 7076; Cell Signaling Technology, Inc.) for 1 h at room temperature. Following washing signals, were detected by chemiluminescence using western blotting luminol reagent (Santa Cruz Biotechnology, Inc.). Protein levels were quantified by scanning blots on a Gel Doc EZ imager (Bio-Rad Laboratories, Inc.) and analysis with Quantity One 1D image analysis software 4.4.0 (Bio-Rad Laboratories, Inc.).

Statistical analysis. All statistical analyses were performed using SPSS 20.0 (IBM Corp.). Medcalc v18.9 (Medcalc Software Bvba) software was used to calculate the sample size to ensure that it was sufficient to detect the pre-specified effect amount. To determine the significant difference, Student's t-test was used for comparison between the two groups and one-way analysis of variance was used for comparison of multiple groups. Bonferroni's was used as a post hoc test. The Fisher's exact test was used to test the association between the two categorical variables. Each experiment was repeated at least three times. In Kaplan-Meier curves survival analysis, log-rank test was used. $P<0.05$ was considered to indicate a statistically significant difference.

Results

Profiling and characteristics of exosomal circRNAs in patients with LC following TACE. patients with LC were enrolled from the affiliated hospital of Chengdu Medical College between 2018 and 2019. All patients were male, with ages ranging between 26 and 66 years old. Of these patients, four had hepatitis virus B (HBV) infection (Table SII). During the TACE process, cisplatin (50 mg) and fluorouracil (250 mg) were injected into the tumor tissue through the hepatic artery for local chemotherapy and the main blood supply of the tumor was embolized with lipiodol. The tumor and iodized

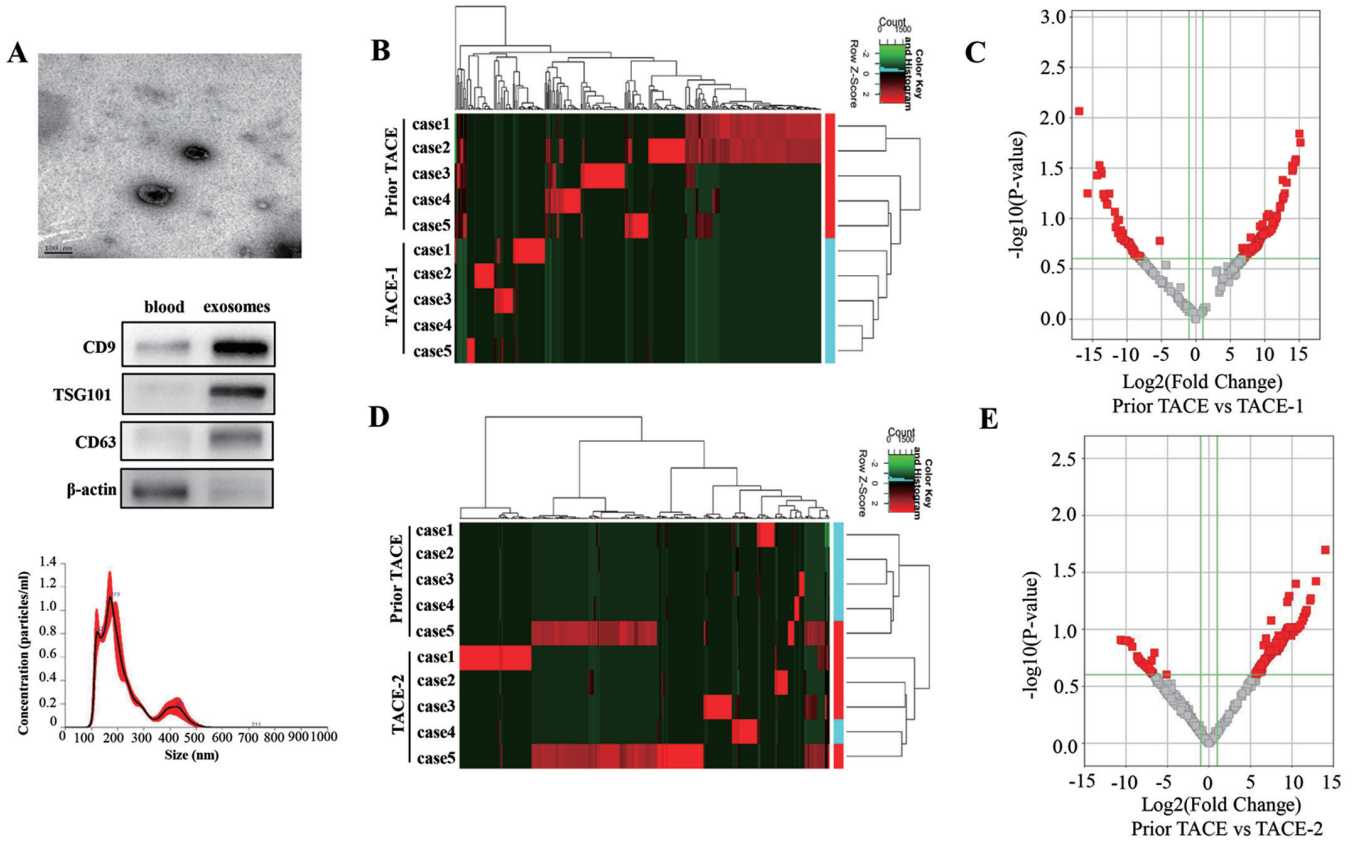

Figure 1. Profiling and characteristics of exosomal circRNAs in patients with LC following TACE. (A) TEM image of exosomes with negative staining to enhance the view of membrane structures (scale bar=100 nm). Western blotting detected CD9, CD63, TSG101 and β-actin in exosomes (blood used as control). Malvern Nano-Nano Analyzer demonstrated the diameter distribution of isolated exosomes. (B) Heat map of 390 differentially expressed circRNAs between prior TACE and TACE1. Each column represents one sample; each row represents one probe set. Red color (upregulated expression) or green (downregulated expression). The dendrogram on the right reveals the sample clustering; the dendrogram on the top reveals the gene clustering. (C) Volcano plot using fold change and P-value. The red rectangle represents differentially expressed circRNAs between prior TACE and TACE1, P<0.05, fold change ≥2.0. (D) Heat map of 489 differentially expressed circRNAs between prior TACE and TACE2. Each column represents one sample; each row represents one probe set. Red color (upregulated expression) or green (downregulated expression). The dendrogram on the right reveals the sample clustering; the dendrogram on the top reveals the gene clustering. (E) Volcano plot using fold change and P-value. The red rectangle represents differentially expressed circRNAs between prior TACE and TACE2, P<0.05, fold change ≥2.0. circRNA, circular RNA; LC, liver cancer; TACE, transarterial chemoembolization; TEM, transmission electron microscope; TACE1, after the first TACE operation; TACE2, after the second TACE operation.

oil deposits observed during treatment are shown in Fig. S1. Through TNM and Barcelona Clinic Liver Cancer staging (BCLC) tumor staging assessment, it was confirmed that following performing TACE twice, case 1, 2 and 3 achieved a partial response and case 4 and 5 achieved a stable disease state (Table SII). In addition, the Child-Pugh score was used to evaluate the changes in liver function of the patients following TACE treatment. The results demonstrated that TACE treatment did not damage the liver function of the patients (Table SII).

Under TEM, the diameter of the exosomes ranged from 30 to 150 nm and the membrane was clear and relatively complete (Fig. 1A). The exosomes expressed typical exosome markers, such as CD9, TSG101 and CD63. However, there was no expression of CD63 and TSG101 and low expression of CD9 in the blood. There was no expression of β-actin in the exosomes (Fig. 1A). The MNNA demonstrated that the peak of the isolated exosomes occurred at approximately 150 nm (Fig. 1A). CircRNA-seq identified 390 differentially expressed circRNAs between the prior TACE and TACE1 groups (fold change ≥2.0; P<0.05). Heat maps of 390 differentially expressed circRNAs were generated to illustrate the distinguishable circRNA expression profile of the samples (Fig. 1B). The volcano plot analysis demonstrated 305 upregulated and 85 downregulated circRNAs (Fig. 1C). Hierarchical cluster analysis clearly identified 489 differentially expressed circRNAs between the TACE and TACE2 groups (Fig. 1D). The volcano plot analysis demonstrated 422 upregulated and 67 downregulated circRNAs (Fig. 1E).

GO analysis of differentially expressed circRNA-derived genes. The GO analysis included three categories: Biological process (BP), cell component (CC) and molecular function (MF). The BP analysis demonstrated that between the prior TACE and TACE1 groups, the differentially expressed circRNAs were significantly associated with myosin filament assembly, negative regulation of androgen receptor and negative regulation of B cells (Fig. 2A and B). Significant CC terms associated with the differentially expressed circRNAs between the prior TACE and TACE1 groups were associated with the myosin filament, nuclear membrane protein complex, immunological synapse and basal plasma membrane (Fig. 2A and B). For MF, the differentially expressed circRNAs between the prior TACE and TACE1 groups were associated with IgG

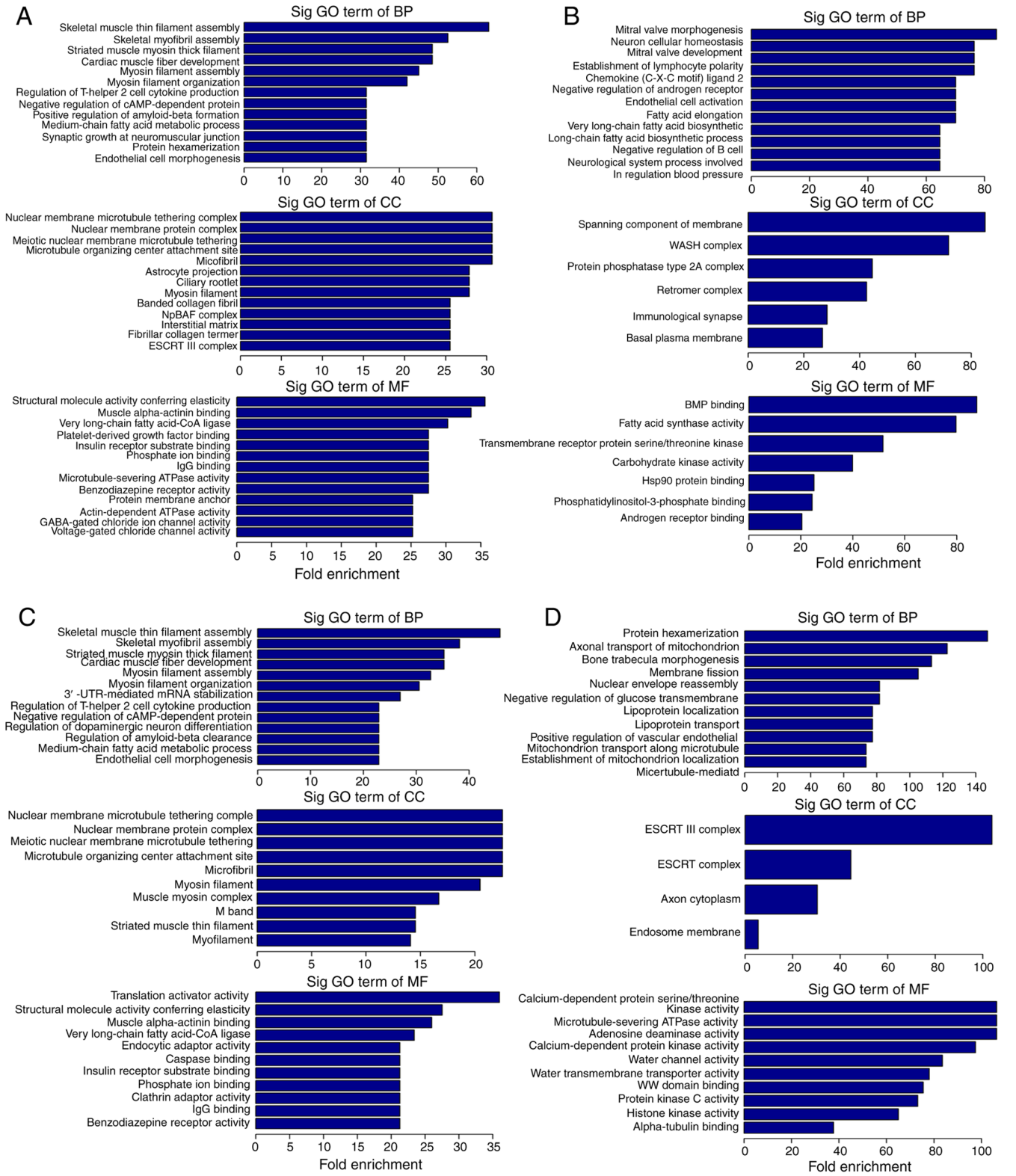

Figure 2. GO analysis of differentially expressed circRNA-derived genes. The horizontal axis is the enrichment score for the GO terms and the vertical axis is the GO terms. The enrichment score was calculated as-log10 (P-value). (A) GO analysis of upregulated circRNAs between prior TACE and TACE1. (B) GO analysis of downregulated circRNAs between prior TACE and TACE1. (C) GO analysis of upregulated circRNAs between prior TACE and TACE2. (D) GO analysis of downregulated circRNAs between prior TACE and TACE2. GO, Gene Ontology; circRNA, circular RNA; TACE, transarterial chemoembolization; TACE1, after the first TACE operation; TACE2, after the second TACE operation; Sig, significant; BP, biological process; CC, cell component; MF, molecular function.

binding, very long-chain fatty acid-CoA ligase and insulin receptor substrate binding (Fig. 2A and B). Between the prior TACE and TACE2 groups, the differentially expressed circRNAs associated with BP were significantly associated with myosin filament assembly, the medium-chain fatty acid metabolic process, membrane fission and lipoprotein

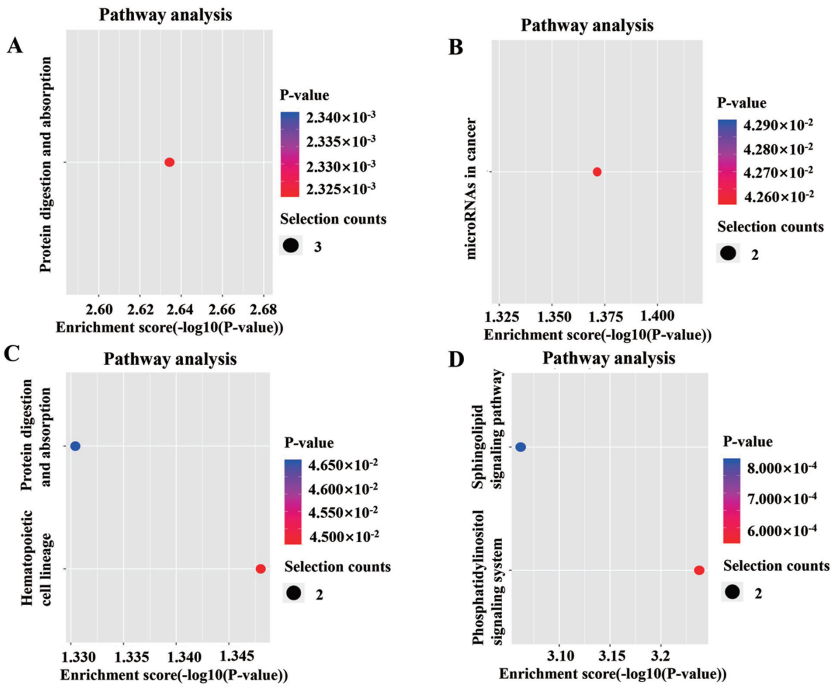

Figure 3. KEGG pathway analysis of differentially expressed circRNA-derived genes. The enrichment score was calculated as-log10 (P-value). Selection counts represent the number of entities of the differentially expressed genes' directly associated with the listed Pathway ID. (A) KEGG pathway analysis of upregulated circRNAs between prior TACE and TACE1. (B) KEGG pathway analysis of downregulated circRNAs between prior TACE and TACE1. (C) KEGG pathway analysis of upregulated circRNAs between prior TACE and TACE2. (D) KEGG pathway analysis of downregulated circRNAs between prior TACE and TACE2. KEGG, Kyoto Encyclopedia of Genes and Genomes; circRNA, circular RNA; TACE, transarterial chemoembolization; TACE1, after the first TACE operation; TACE2, after the second TACE operation; Sig, significant; BP, biological process; CC, cell component; MF, molecular function.

transport (Fig. 2C and D). Significant CC terms associated with the differentially expressed circRNAs were associated with the myosin filament, nuclear membrane protein complex, ESCRT complex and endosome membrane (Fig. 2C and D). For MF, the differentially expressed circRNAs were associated with IgG binding, very long-chain fatty acid-CoA ligase, insulin receptor substrate binding, kinase activity and water channel activity (Fig. 2C and D).

KEGG pathway analysis of differentially expressed circRNA-derived genes. The KEGG pathway dot plot shows the significantly enriched pathways with the enrichment score [-log10 (*P*-value)] values. KEGG pathway analysis predicted the pathways affected by the variations in circRNAs in exosomes from patients with LC following TACE (Fig. 3). Between the TACE and TACE1 groups, the protein digestion and absorption pathway was shown to be activated and the miRNAs involved in the cancer pathway were inhibited (Fig. 3A and B). Pathway analysis demonstrated that between the prior TACE and TACE2 groups, the hematopoietic cell lineage and protein digestion and absorption pathways were both upregulated and the sphingolipid signaling and phosphatidylinositol signaling system pathways were downregulated (Fig. 3C and D).

Circ-G004213 promotes the cisplatin sensitivity of HepG2 cells and improves survival in vivo. To identify the circRNAs that demonstrated significant and consistent changes during TACE treatment, the intersection of the circRNAs with significant changes (fold change >10, P<0.01) were selected for prior TACE vs. TACE2 and TACE vs. TACE2 (Fig. 4A). It was found that circ-G004213 and circ_GABRG3 were upregulated during TACE treatment (Fig. S2A and B). Because the sensitivity of LC cells to cisplatin is significantly associated with the effect of TACE treatment, the expression of circ-G004213 and circ_GABRG3 was detected in HepG2 and cisplatin-resistant HepG2/CIS cells. Notably, as shown in Fig. 4B, circ-G004213 was weakly expressed in HepG2/CIS cells. In addition, circ-G004213 was downregulated by CIS induction (Fig. 4C). Overexpressing and knockout of circ-G004213 was constructed in HepG2 cells (Fig. S3A). To further determine the exact role of circ-G004213 in the sensitivity to CIS, we measured the IC_{50} of CIS in HepG2 cells. As shown in Fig. 4D, overexpression of circ-G004213 enhanced the sensitivity of HepG2 cells to CIS. By contrast, knockout of circ-G004213 increased the tolerance of HepG2 cells to CIS (Fig. 4D). CIS (10 μM) was injected intraperitoneally; circ-G004213 overexpression reduced tumor growth and circ-G004213 knockout increased tumor growth *in vivo* (Fig. 4E). In addition, the survival rate of each group was recorded. As shown in Fig. 4F, treatment with CIS prolonged the survival rate of the circ-G004213-overexpressing cells, but a shorter survival rate was observed in the circ-G004213 knockdown cells compared with the control cells.

Circ-G004213 regulates CIS sensitivity via regulation of miR-513b-5p/PRPR39. CircRNAs can act as miRNA sponges to regulate the expression levels of other related RNAs via miRNA response elements. miRNAs bind to mRNAs to inhibit post-transcriptional gene expression. Based on the first five predicted miRNA targets of circ-G004213 and the first five predicted mRNA targets of each miRNA, the circRNA-miRNA-mRNA network was constructed (Fig. 5A).

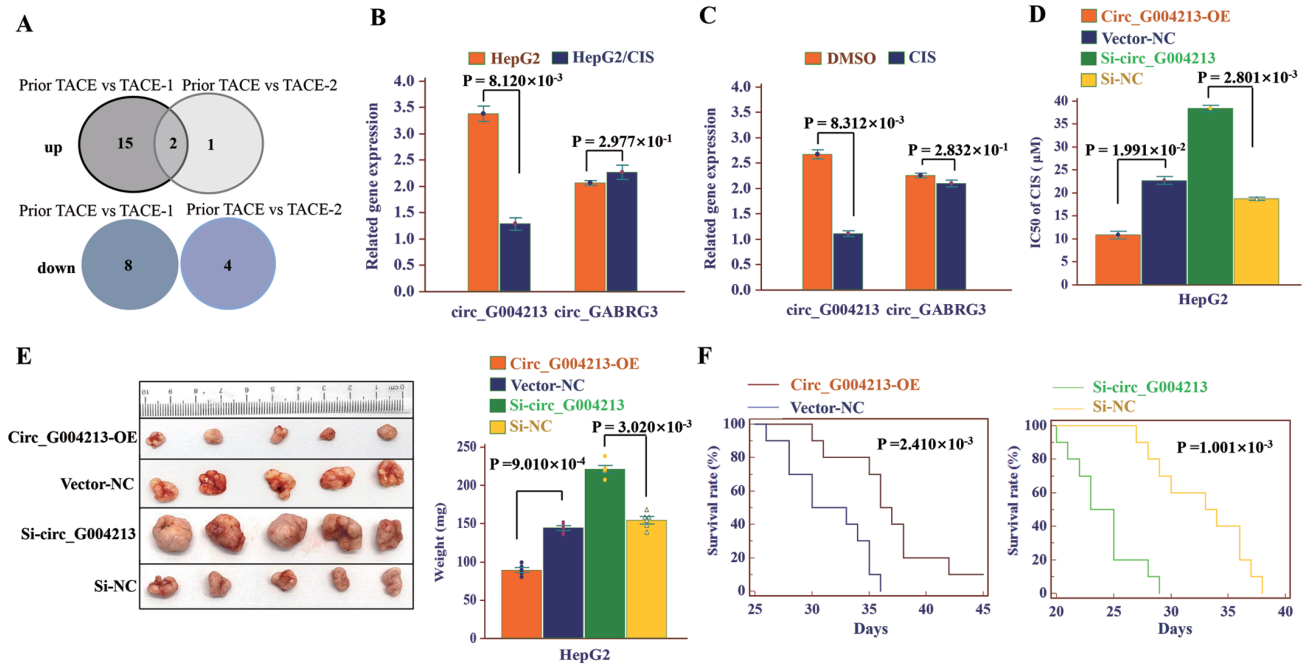

Figure 4. Circ-G004213 promotes the cisplatin sensitivity of HepG2 cells and improves survival *in vivo*. (A) A Venn diagram demonstrated the intersection of the circRNAs with significant changes (fold change >10; P<0.01) between prior TACE vs. TACE2 and prior TACE vs. TACE2. (B) RT-qPCR detection of circ-G004213 and circ_GABRG3 expression in the cisplatin-resistant cell line HepG2/CIS compared with HepG2. (C) RT-qPCR detection of circ-G004213 and circ_GABRG3 expression, when HepG2 cells were treated with CIS (10 μM) for 3 days. (D) circ-G004213 overexpressing (circ-G004213-OE), negative control (Vector-NC), circ-G004213 knockout (si-circ-G004213) and control (si-NC) HepG2 cells were treated with gradually increasing concentrations of CIS for 3 days and the IC_{50} values of CIS were compared among the groups. (E) Volume and weight of the tumor. (F) When mice succumbed, the survival time of each group was recorded and the Kaplan-Meier survival curves for each group were analyzed (n=10 per group). circRNA, circular RNA; TACE, transarterial chemoembolization; TACE1, after the first TACE operation; TACE2, after the second TACE operation; CIS, cisplatin; RT-qPCR, reverse transcription-quantitative PCR; si, short interfering.

miR-513b-5p was significant and continued to decrease following TACE, so it was selected for further analysis (Fig. 5B). Luciferase reporter analysis was used to determine whether miR-513b-5p was directly targeted by circ-G004213. A double luciferase reporter vector was constructed containing full-length WT circ-G004213 or a version where the miR-513b-5p-binding site was mutated (Fig. 5C). A significant decrease in luciferase reporter activity was detected in the 293T cells cotransfected with miR-513b-5p mimic and WT but not the mutant vector (Fig. 5D). Overexpressing and knockout of miR-513b-5p was constructed in HepG2 cells (Fig. S3B). In summary, these experiments demonstrated that circ-G004213 can be used as a sponge for miR-513b-5p and the miR-513b-5p inhibitor can improve the sensitivity of HepG2 cells to CIS (Fig. 5E). By contrast, miR-513b-5p mimics increased HepG2 tolerance to CIS (Fig. 5E).

PRPF39, as a predicted mRNA target of miR-513b-5p, was significantly upregulated following TACE (Fig. S2C) and associated with cisplatin resistance (15). The roles of PRPF39 were determined in CIS sensitivity. Overexpressing and knockout of PRPF39 was constructed in HepG2 cells (Fig. S3C). As shown in Fig. 5F, PRPF39 overexpression enhanced the sensitivity of HepG2 cells to CIS. PRPF39 knockdown increased the tolerance of HepG2 to CIS (Fig. 5F). The present study found that the miR-513b-5p inhibitor increased PRPF39 expression, while the miR-513b-5p mimic decreased PRPF39 expression (Fig. 5G). According to MRE analysis, miR-513b-5p had two potential binding sites in the 3'UTR of PRPF39 (Fig. 5H). Therefore, luciferase reporter plasmids containing the WT and mutated 3'UTR of PRPF39 were designed to predict the binding site. Following cotransfection of the miR-513b-5p mimic with the PRPF39 3'UTR WT1 or PRPF39 3'UTR WT2, the luciferase activity was significantly decreased. The mutant PRPF39 structure was unaffected by miR-513b-5p (Fig. 5I).

The expression of miR-513b-5p and PRPF39 was detected in HepG2 transplanted tumors. The present study demonstrated that the expression of miR-513b-5p was decreased and the expression of PRPF39 was increased in tumor tissues with overexpression of circ-G004213 (Fig. S3C and D). Meanwhile, the expression of miR-513b-5p in tumor tissues was decreased and the expression of PRPF39 was increased in tumor tissues with knockout of circ-G004213 (Fig. S3C and D). These results further demonstrated that circ-G004213 regulated CIS sensitivity by regulating miR-513b-5p/PRPR39.

Circ-G004213 is associated with the prognosis of patients with LC following TACE. The circ-G004213 gene was significantly upregulated following TACE treatment (Fig. S2A), especially for case 1, 2 and 3, which demonstrated an improved prognosis. To further verify the effect of circ-G004213 on the prognosis of patients with LC, the clinicopathological variables and circ-G004213 expression was analyzed in 50 patients with LC following TACE. The results demonstrated that high expression of circ-G004213 was negatively associated with advanced TNM stage, BCLC stage or α-fetoprotein (AFP) and exhibited no significant associations with other parameters, including age, sex, HBV or Child-Pugh score (Table I). Among the mRNAs that were negatively associated with the prognosis of

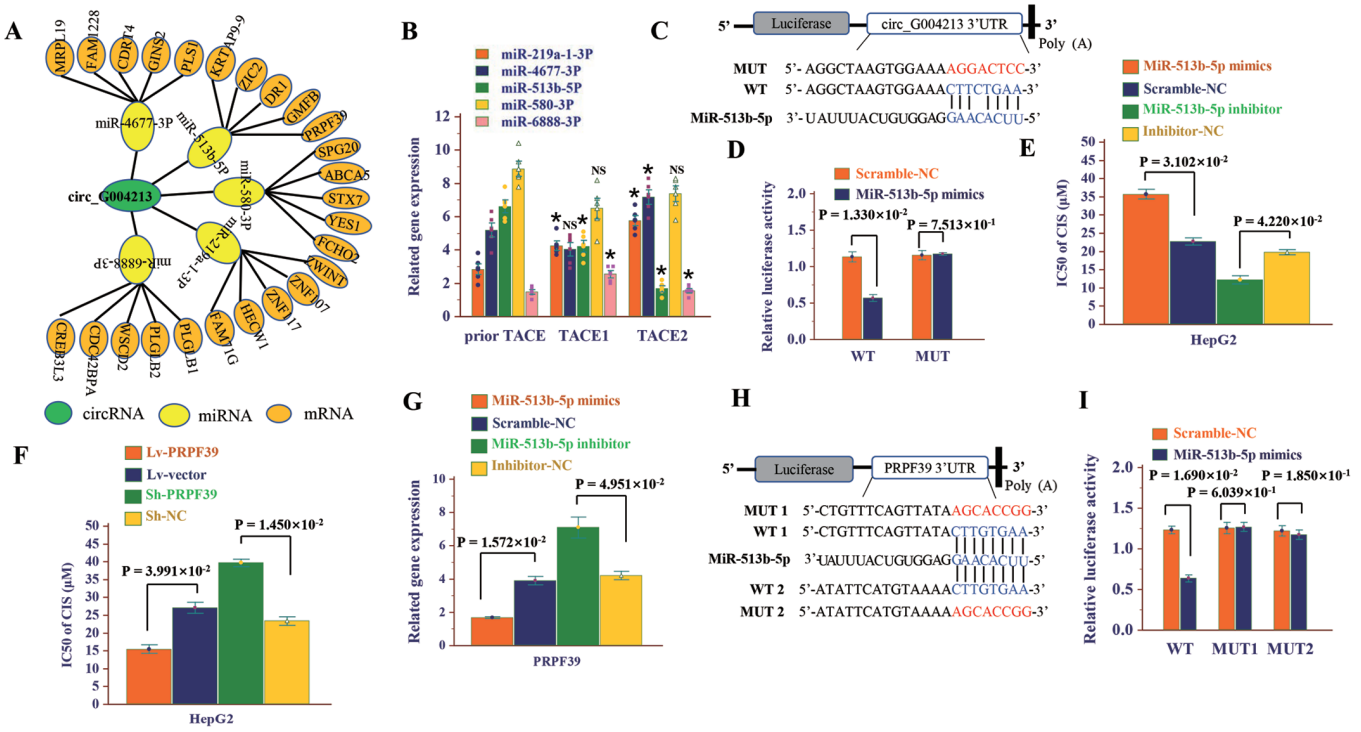

Figure 5. Circ-G004213 regulates CIS sensitivity via regulation miR-513b-5p/PRPR39. (A) CircRNA-miRNA-mRNA network analysis. (B) The five miRNAs most highly ranked as the candidate miRNAs during TACE treatment. Triangles or circles represent samples in different groups, *P<0.05 and NS vs. the corresponding samples of the prior TACE group. (C) A schematic of WT and MUT circ-G004213 luciferase reporter vectors. (D) The luciferase activity of WT circ-G004213 3'UTR or mutant circ_0025202 3' UTR following transfection with miR-513b-5P mimics in 293T cells. (E) HepG2 cells transfection with miR-513b-5P mimics, mimics-NC, miR-513b-5P inhibitor and inhibitor-NC were treated with gradually increasing concentrations of CIS for three days and the IC_{50} values of CIS were compared among the groups. (F) PRPF39 overexpressing (lv-PRPF39), control (lv-vector), PRPF39 knockout (sh-PRPF39) and control (sh-NC) HepG2 cells were treated with CIS and the IC_{50} values of CIS compared. (G) PRPF39 in miR-513b-5P mimics, mimics-NC, miR-513b-5P inhibitor and inhibitor-NC groups. (H) Potential binding sites of miR-513b-5P with PRPF39 3'UTR. (I) The luciferase activity of WT PRPF39 3'UTR or mutant PRPF39 3'UTR of two potential binding sites following transfection with miR-513b-5P mimics in 293T cell lines. Data are presented as means ± SEM of at least three independent experiments. CIS, cisplatin; miRNA, microRNA; circRNA, circular RNA; NS, no significant difference; WT, wild-type; MUT, mutant; UTR, untranslated region; sh, short hairpin.

patients, the downstream mRNAs of circ-G004213, GINS2, ZIC2 and CREB3L3 were significantly downregulated following TACE (Fig. S2D) and the mRNAs positively associated with patient prognosis, PRPF39 and ZWINT, were significantly upregulated following TACE (Fig. S2C). The above results suggested that the expression of circ-G004213 in exosomes may be positively associated with the prognosis of patients with LC following TACE.

Discussion

Exosomes serve a crucial role in the carcinogenesis of LC. In particular, small noncoding RNAs in exosomes could serve as biomarkers for the prediction and diagnosis of LC (27). Exosomes from LC cells can promote the occurrence and development of LC. For example, Exosomes derived from HepG2 cell can reprogram biological behaviors of LO2 cells (28) and exosomes derived from LC patient serum and HepG2 cells can inhibit proliferation and sorafenib chemoresistance in LC (29).

Recently, an increasing number of studies have demonstrated that exosomal circRNAs serve a crucial role in the prediction and diagnosis of LC (10-13). Exosomal circPTGR1 from cells with high metastatic (LM3) can promote LC metastasis via the miR449a-MET pathway (17). Although TACE is an important treatment for LC, the alteration and effects of circRNAs in LC following TACE remain to be elucidated. The alterations of the expression profile of circRNAs in exosomes from patients with LC following TACE were studied for the first time, to the best of the authors' knowledge, by high-throughput whole transcriptome sequencing and subsequent bioinformatic analysis in the present study.

The present study identified 390 differentially expressed circRNAs between the prior TACE and TACE1 groups and 489 differentially expressed circRNAs between the prior TACE and TACE2 groups. Based on these different circRNAs, GO analysis was performed to annotate and determine the function of these circRNAs. The present study demonstrated that they were associated with fatty acid metabolism, receptor binding and membrane protein complexes. The medium-chain fatty acid metabolic process is associated with the metabolism, metastasis and prognosis of LC (30,31). The insulin receptor is associated with LC cell viability and proliferation (32). The nuclear membrane protein complex promotes the early recurrence of hepatocellular carcinoma in association with the Wnt/β-catenin signaling pathway (33). KEGG pathway analysis predicted that protein digestion and absorption pathways were activated following TACE. This pathway is associated with the anti-LC efficacy of DHA in combination with sorafenib (34).

To identify the circRNAs that demonstrated significant and consistent changes during TACE treatment, the

intersection of the circRNAs with significant changes for prior TACE vs. TACE2 and TACE vs. TACE2 were selected. It was found that circ-G004213 and circ_GABRG3 were upregulated during TACE treatment. Cisplatin is a common chemotherapeutic agent in TACE. Therefore, the sensitivity of cisplatin chemotherapy is an important factor affecting TACE treatment. The expression of circ-G004213 and circ_GABRG3 was detected in HepG2 and cisplatin-resistant HepG2/CIS cells. The present study demonstrated that circ-G004213 was expressed at low levels in HepG2/CIS cells and downregulated in response to CIS induction. However, the role and mechanism of circ_GABRG3 in TACE require further study. Further analysis confirmed that circ-G004213 promoted the cisplatin sensitivity of HepG2 cells and improved survival *in vivo*.

Bioinformatic analysis has shown that some circRNAs can act as miRNA sponges to regulate the expression levels of other related RNAs via miRNA response elements. This mechanism is called competitive endogenous RNA mechanism. miRNAs bind to mRNAs to inhibit post-transcriptional gene expression and serve an important role in regulating gene expression, the cell cycle and organismal development (35). Therefore, it is important to identify the interactions of circRNAs, miRNAs and mRNAs. Based on the first five predicted miRNA targets and the first five predicted mRNA targets of each miRNA, the circRNA-miRNA-mRNA network was constructed. Among the predicted miRNAs, miR-513b-5p was confirmed to be a candidate miRNA. miR-513b-5p is associated with cell proliferation and migration in ovarian cancer (20). Furthermore, the present study confirmed that PRPF39, as a mRNA target of miR-513b-5p, was significantly upregulated following TACE. Knockdown of PRPF39 expression using siRNA resulted in a significant increase in cisplatin resistance (21). Therefore, circ-G004213 regulates CIS sensitivity via miR-513b-5p/PRPR39.

Studies demonstrate that exosomes from HCC cells can promote the occurrence and development of LC (28,29). However, the present study used HepG2 cells for the purpose of elucidating the role of circ-G004213 in cisplatin chemotherapy and further proved the interaction of circ-G004213/miR-513b-5p/PRPF39. Therefore, it did not isolate exosomes from HepG2 cells for further study. However, in a future study, will further analyze the role of exosomal circRNAs source of HepG2 cells on cisplatin chemotherapy.

The present study demonstrated that high expression of circ-G004213 was negatively associated with advanced TNM stage, BCLC stage or AFP and exhibited no significant associations with other parameters, including age, sex, HBV or Child-Pugh score. TNM stage, BCLC stage and AFP predict poor prognosis in patients with LC (36-38). It was found that potential downstream mRNAs of circ-G004213, GINS2, ZIC2 and CREB3L3 were significantly downregulated and PRPF39 and ZWINT were significantly upregulated following TACE. The upregulation and interrelated expression of GINS subunits predicts poor prognosis in patients with LC (39). ZIC2 could promote tumor growth and metastasis via PAK4 in LC (40). ZIC2-dependent octamer-binding transcription factor 4 activation drives the self-renewal of human LC stem cells (41). CREBH, which is activated by stress in the endoplasmic reticulum (ER), is an ER-resident transmembrane basic leucine zipper (bZIP) transcription factor that is specifically expressed in the liver and activated CREBH may serve an important role in LC proliferation (42). Therefore, GINS2, ZIC2 and CREB3L3 were negatively associated with the prognosis of LC. Knockdown of PRPF39 expression using siRNA results in a significant increase in cisplatin resistance (21) and cisplatin is the main chemotherapy drug used for TACE. Overexpression of ZWINT predicts poor prognosis and promotes the proliferation of LC by regulating cell cycle-related proteins (43). Therefore, PRPF39 and ZWINT were positively associated with the prognosis of LC and circ-G004213 was positively associated with the prognosis of LC.

In conclusion, the above results suggested that the expression of circ-G004213 in exosomes could promote CIS sensitivity via regulation of miR-513b-5p/PRPR39 and circ-G004213 was positively associated with the prognosis of patients with LC following TACE. Circ-G004213 may be an indicator for predicting the efficacy of TACE in patients with LC.

Acknowledgements

Not applicable.

Funding

The present study was supported by grants from the National Natural Science Foundation of China (grant no. 81702446), Department education of Sichuan Province (grant nos. 18ZA0151 and 18ZB0175), Department of Science and Technology of Sichuan Province (grant no. C2018JY0654), Fund of Chengdu Medical College (grant no. CDYXY007) and Special Research Fund of the First Affiliated Hospital of Chengdu Medical College (grant no. CYFY2017YB09).

Availability of data and materials

The datasets generated and/or analyzed during the current study are available in the Gene Expression Omnibus repository at https://www.ncbi.nlm.nih.gov/geo/ query/acc.cgi?acc=GSE165183.

Authors' contributions

LQ was mainly involved in patient recruitment, TACE treatment and clinical sample collection. ZZ was involved in clinical data collection and analysis. CW performed the animal experiment. XL was involved in clinic sample storage and processing. TZ was involved in sequencing data analysis and drug resistance experiment. JL mainly contributed to designing and performing the present study and manuscript editing. LQ and JL were responsible for the authenticity of the data in this article. All authors reviewed and approved the final manuscript.

Ethics approval and consent to participate

Informed consent was signed in writing by all patients and the study protocol was approved by the ethics committee of the

First Affiliated Hospital of Chengdu Medical College (approval no. 2017009). The animal experiments were approved by the research ethics committee of Chengdu Medical College (approval no. 2017CYA-021).

Patient consent for publication

Not applicable.

Competing interests

The authors declare that they have no competing interests.

References

1. Lingiah VA, Niazi M, Olivo R, Paterno F, Guarrera JV and Pyrsopoulos NT: Liver transplantation beyond milan criteria. J Clin Transl Hepatol 8: 69-75, 2020.
2. Wu CC, Ho WL and Liu TJ: Hepatocellular carcinoma with adjacent organ extension: The enhancement of preoperative transcatheter arterial embolization and the results of surgical resection. Surg Today 24: 882-888, 1994.
3. Grandhi MS, Kim AK, Ronnekleiv-Kelly SM, Kamel IR, Ghasebeh MA and Pawlik TM: Hepatocellular carcinoma: From diagnosis to treatment. Surg Oncol 25: 74-85, 2016.
4. Gu J, Zhang X, Cui R, Zhang J, Wang Z, Jia Y, Miao R, Dong Y, Ma X, Fan H, *et al*: Prognostic predictors for patients with hepatocellular carcinoma receiving adjuvant transcatheter arterial chemoembolization. Eur J Gastroenterol Hepatol 31: 836-844, 2019.
5. Loosen SH, Schulze-Hagen M, Leyh C, Benz F, Vucur M, Kuhl C, Trautwein C, Tacke F, Bruners P, Roderburg C and Luedde T: IL-6 and IL-8 serum levels predict tumor response and overall survival after TACE for primary and secondary hepatic malignancies. Int J Mol Sci 19: 1766, 2018.
6. Daniele A, Divella R, Quaranta M, Mattioli V, Casamassima P, Paradiso A, Garrisi VM, Gadaleta CD, Gadaleta-Caldarola G, Savino E, *et al*: Clinical and prognostic role of circulating MMP-2 and its inhibitor TIMP-2 in HCC patients prior to and after trans-hepatic arterial chemo-embolization. Clin Biochem 47: 184-190, 2014.
7. Zhou L, Lv T, Zhang Q, Zhu Q, Zhan P, Zhu S, Zhang J and Song Y: The biology, function and clinical implications of exosomes in lung cancer. Cancer Lett 407: 84-92, 2017.
8. Shi X, Wang B, Feng X, Xu Y, Lu K and Sun M: circRNAs and exosomes: A mysterious frontier for human cancer. Mol Ther Nucleic Acids 19: 384-392, 2020.
9. Wan M, Ning B, Spiegel S, Lyon CJ and Hu TY: Tumor-derived exosomes (TDEs): How to avoid the sting in the tail? Med Res Rev 40: 385-412, 2020.
10. Han Q, Zhao H, Jiang Y, Yin C and Zhang J: HCC-derived exosomes: Critical player and target for cancer immune escape. Cells 8: 558, 2019.
11. Abudoureyimu M, Zhou H, Zhi Y, Wang T, Feng B, Wang R and Chu X: Recent progress in the emerging role of exosome in hepatocellular carcinoma. Cell Prolif 52: e12541, 2019.
12. Sarnow P and Sagan SM: Unraveling the mysterious interactions between hepatitis C virus RNA and liver-specific microRNA-122. Annu Rev Virol 3: 309-332, 2016.
13. Li B, Mao R, Liu C, Zhang W, Tang Y and Guo Z: LncRNA FAL1 promotes cell proliferation and migration by acting as a CeRNA of miR-1236 in hepatocellular carcinoma cells. Life Sci 197: 122-129, 2018.
14. Liu J, Fan L, Yu H, Zhang J, He Y, Feng D, Wang F, Li X, Liu Q, Li Y, *et al*: Endoplasmic reticulum stress causes liver cancer cells to release exosomal miR-23a-3p and up-regulate programmed death ligand 1 expression in macrophages. Hepatology 70: 241-258, 2019.
15. Huang XY, Huang ZL, Huang J, Xu B, Huang XY, Xu YH, Zhou J and Tang ZY: Exosomal circRNA-100338 promotes hepatocellular carcinoma metastasis via enhancing invasiveness and angiogenesis. J Exp Clin Cancer Res 39: 20, 2020.
16. Su Y, Lv X, Yin W, Zhou L, Hu Y, Zhou A and Qi F: CircRNA Cdr1as functions as a competitive endogenous RNA to promote hepatocellular carcinoma progression. Aging (Albany NY) 11: 8182-8203, 2019.
17. Wang G, Liu W, Zou Y, Wang G, Deng Y, Luo J, Zhang Y, Li H, Zhang Q, Yang Y and Chen G: Three isoforms of exosomal circPTGR1 promote hepatocellular carcinoma metastasis via the miR449a-MET pathway. EBioMedicine 40: 432-445, 2019.
18. Zhang H, Deng T, Ge S, Liu Y, Bai M, Zhu K, Fan Q, Li J, Ning T, Tian F, *et al*: Exosome circRNA secreted from adipocytes promotes the growth of hepatocellular carcinoma by targeting deubiquitination-related USP7. Oncogene 38: 2844-2859, 2019.
19. Wang X, Zhang X, Wang G, Wang L, Lin Y and Sun F: Hsa-miR-513b-5p suppresses cell proliferation and promotes P53 expression by targeting IRF2 in testicular embryonal carcinoma cells. Gene 626: 344-353, 2017.
20. Lin W, Ye H, You K and Chen L: Up-regulation of circ_LARP4 suppresses cell proliferation and migration in ovarian cancer by regulating miR-513b-5p/LARP4 axis. Cancer Cell Int 20: 5, 2020.
21. Stark AL, Delaney SM, Wheeler HE, Im HK and Dolan ME: Functional consequences of PRPF39 on distant genes and cisplatin sensitivity. Hum Mol Genet 21: 4348-4355, 2012.
22. National Health and Family Planning Commission. Notice of general office of national health and family planning commission on printing and issuing standards for diagnosis and treatment of primary liver cancer (2017 edition). http://www.nhfpc.gov.cn/yzygj/s7659/201706/80abf02a86c048fcd 130 e5e298f7aeee.shtml. Accessed June 2, 2017.
23. Kim KM, Shim SG, Sinn DH, Song JE, Kim BS and Kim HG: Child-Pugh, MELD, MELD-Na, and ALBI scores: Which liver function models best predicts prognosis for HCC patient with ascites? Scand J Gastroenterol 55: 951-957, 2020.
24. Li K, Gao B, Li J, Chen H, Li Y, Wei Y, Gong D, Gao J, Zhang J, Tan W, *et al*: ZNF32 protects against oxidative stress-induced apoptosis by modulation C1QBP transcription. Oncotarget 6: 38107-38126, 2015.
25. Li J, Ao J, Li K, Zhang J, Li Y, Zhang L, Wei Y, Gong D, Gao J, Tan W, *et al*: ZNF32 contributes to the induction of multidrug resistance by regulating TGF-β receptor 2 signaling in lung adenocarcinoma. Cell Death Dis 7: e2428, 2016.
26. Livak KJ and Schmittgen TD: Analysis of relative gene expression data using real-time quantitative PCR and the 2(-Delta Delta C(T)) method. Methods 25: 402-408, 2001.
27. Wang H, Lu Z and Zhao X: Tumorigenesis, diagnosis, and therapeutic potential of exosomes in liver cancer. J Hematol Oncol 12: 133, 2019.
28. He X, Yu J, Xiong L, Liu Y, Fan L, Li Y, Chen B, Chen J and Xu X: Exosomes derived from liver cancer cells reprogram biological behaviors of LO2 cells by transferring Linc-ROR. Gene 719: 144044, 2019.
29. Wang G, Zhao W, Wang H, Qiu G, Jiang Z, Wei G and Li X: Exosomal miR-744 inhibits proliferation and sorafenib chemoresistance in hepatocellular carcinoma by targeting PAX2. Med Sci Monit 25: 7209-7217, 2019.
30. Wakana H, Kono H, Fukushima H, Nakata Y, Akazawa Y, Maruyama S, Hagio K, Fujii H and Ichikawa D: Effects of medium-chain triglycerides administration in chemically-induced carcinogenesis in mice. Anticancer Res 39: 6653-6660, 2019.
31. Wang H, Lu J, Dolezal J, Kulkarni S, Zhang W, Chen A, Gorka J, Mandel JA and Prochownik EV: Inhibition of hepatocellular carcinoma by metabolic normalization. PLoS One 14: e0218186, 2019.
32. Sakurai Y, Kubota N, Takamoto I, Obata A, Iwamoto M, Hayashi T, Aihara M, Kubota T, Nishihara H and Kadowaki T: Role of insulin receptor substrates in the progression of hepatocellular carcinoma. Sci Rep 7: 5387, 2017.
33. Chen J, Rajasekaran M, Xia H, Zhang X, Kong SN, Sekar K, Seshachalam VP, Deivasigamani A, Goh BK, Ooi LL, *et al*: The microtubule-associated protein PRC1 promotes early recurrence of hepatocellular carcinoma in association with the Wnt/β-catenin signalling pathway. Gut 65: 1522-1534, 2016.
34. Hou C, Guo D, Yu X, Wang S and Liu T: TMT-based proteomics analysis of the anti-hepatocellular carcinoma effect of combined dihydroartemisinin and sorafenib. Biomed Pharmacother 126: 109862, 2020.
35. Cao D, Wang Y, Li D and Wang L: Reconstruction and analysis of the differentially expressed lncRNA-miRNA-mRNA network based on competitive endogenous RNA in hepatocellular carcinoma. Crit Rev Eukaryot Gene Expr 29: 539-549, 2019.
36. Zhou ZR, Liu M, Lu HR, Li YF, Liang SX and Zhang CY: Validation of different staging systems for hepatocellular carcinoma in a cohort of 249 patients undergoing radiotherapy. Oncotarget 8: 46523-46531, 2017.

37. de Freitas LB, Longo L, Santos D, Grivicich I and Álvares-da-Silva MR: Hepatocellular carcinoma staging systems: Hong Kong liver cancer vs Barcelona clinic liver cancer in a Western population. World J Hepatol 11: 678-688, 2019.
38. Bird TG, Dimitropoulou P, Turner RM, Jenks SJ, Cusack P, Hey S, Blunsum A, Kelly S, Sturgeon C, Hayes PC and Bird SM: Alpha-fetoprotein detection of hepatocellular carcinoma leads to a standardized analysis of dynamic AFP to improve screening based detection. PLoS One 11: e0156801, 2016.
39. Lian YF, Li SS, Huang YL, Wei H, Chen DM, Wang JL and Huang YH: Up-regulated and interrelated expressions of GINS subunits predict poor prognosis in hepatocellular carcinoma. Biosci Rep 38: BSR20181178, 2018.
40. Lu SX, Zhang CZ, Luo RZ, Wang CH, Liu LL, Fu J, Zhang L, Wang H, Xie D and Yun JP: Zic2 promotes tumor growth and metastasis via PAK4 in hepatocellular carcinoma. Cancer Lett 402: 71-80, 2017.
41. Zhu P, Wang Y, He L, Huang G, Du Y, Zhang G, Yan X, Xia P, Ye B, Wang S, *et al*: ZIC2-dependent OCT4 activation drives self-renewal of human liver cancer stem cells. J Clin Invest 125: 3795-3808, 2015.
42. Cho HK, Kim SY, Kyaw YY, Win AA, Koo SH, Kim HH and Cheong J: HBx induces the proliferation of hepatocellular carcinoma cells via AP1 over-expressed as a result of ER stress. Biochem J 466: 115-121, 2015.
43. Ying H, Xu Z, Chen M, Zhou S, Liang X and Cai X: Overexpression of Zwint predicts poor prognosis and promotes the proliferation of hepatocellular carcinoma by regulating cell-cycle-related proteins. Onco Targets Ther 11: 689-702, 2018.